

Fingertip force control based on max torque adjustment for dexterous manipulation of an anthropomorphic hand

Kien-Cuong Nguyen and Véronique Perdereau

Abstract—Despite recent progress, the performance of force control algorithms still appears to be poor when applying to systems with significant backlash, low precision of position sensors, low communication bandwidth and computation power. Anthropomorphic robot hands with tendon driven joints are typical examples of such systems. To overcome this difficulty, this paper proposes an approach that uses the torque saturation (max-torque) of the joint position control loops to control the end-effector (fingertip) force. This control scheme has been implemented and tested on the Shadow motor robot hand. An application of this control scheme has also been implemented for two fingers holding and rotating an object around the vertical axis. This experiment shows the strong potential of this force control algorithm for grasping and dexterous manipulation activities.

I. INTRODUCTION

In robotics, force control seems to be a well "mastered" subject with many works that have been done up-to-date [1], [2]. However, if we take a closer look to these works, most of them are for industrial robot manipulators, not for anthropomorphic robot hands. Yet the last ones have many characteristics different from those of classical robot manipulators:

- low precision of position sensors (and hence repeatability): due to small size of joints, highly precise joint angle sensors (usually big in size) cannot be integrated but those typically of around 0.2° [3]. Consequently, the repeatability at the fingertip is around 0.4mm, much less than the repeatability at the end-effector of industrial robot arms.
- significant backlash and dry friction: tendon driven joints are a natural solution for making robot hand size similar to the one of the human hand while still maintaining comparable exerting forces. However, this type of joints usually suffers from significant backlash and dry friction on the tendon path [4].
- low communication bandwidth and computation power: anthropomorphic robot hands are usually designed as embedded devices. Consequently, the communication bandwidth and computation power are quite limited. This gives additional constraints to the controller implementation.

These differences make classical force control algorithms perform poorly when applied to anthropomorphic robot

UPMC Univ Paris 06, UMR7222, ISIR, F-75005, Paris, France, kien-cuong.nguyen@upmc.fr

The research leading to these results has been supported by the HANDLE project, which has received funding from the European Community's Seventh Framework Programme (FP7/2007-2013) under grant agreement ICT 231640.

hands. More attention should then be paid to the force control of this kind of effectors, especially when we want them to perform dexterous manipulation.

In this paper, we concentrate our efforts on the fingertip force control of an anthropomorphic robot hand with double acting N -type tendon-driven joints [4]. This class of joints is widely used in anthropomorphic hands (UB hand [5], Salisbury hand [6], DIST hand [7] and recently the Shadow motor hand [8]) thanks to its compactness, intuitive control structure and energy efficiency. However, this kind of joints suffers from significant backlash [4] and this backlash drastically reduces the fingertip force control performance.

A novel solution using max-torque adjustment is proposed in section IV to overcome this difficulty. Before going any further, a detailed description of the notations and hypothesis is given in section II. Classical approaches of force control is given in section III. The experimental validation is presented in section V. An application of this force controller is given in section VI. Finally come the conclusion and future works in section VII.

II. NOTATIONS AND HYPOTHESIS

In this section, only one finger is considered. This finger has from three to five degrees of freedom and is supposed to have contacts with other objects at the fingertip only (fig. 1(a) and 1(b)).

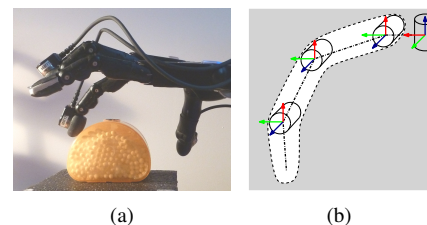


Fig. 1. (a) Studied robot hand and (b) first finger kinematics

The equation of motion of such finger is given by:

$$\mathbf{B}(\mathbf{q})\ddot{\mathbf{q}} + \mathbf{C}(\mathbf{q}, \dot{\mathbf{q}})\dot{\mathbf{q}} + \mathbf{F}\dot{\mathbf{q}} + \mathbf{g}(\mathbf{q}) = \boldsymbol{\tau}_a - \boldsymbol{\tau}_{fr} - \mathbf{J}^T(\mathbf{q})\mathbf{F}_c \quad (1)$$

where \mathbf{q} is the vector of joint angles, $\mathbf{B}(\mathbf{q})$ is the inertia matrix, $\mathbf{C}(\mathbf{q}, \dot{\mathbf{q}})$ is the matrix representing the Coriolis effect and centrifugal forces, \mathbf{F} is the viscous friction coefficient, $\mathbf{g}(\mathbf{q})$ is the vector representing the gravitational effect, $\boldsymbol{\tau}_a$ is the actuating joint torque, $\boldsymbol{\tau}_{fr}$ is the joint friction, \mathbf{F}_c is the contact force at the fingertip and \mathbf{J} is the Jacobian matrix of the finger kinematics.

Even though a robot finger is kinematically similar to an robot manipulator, it is much lighter ($\sim 20\text{g}$) with small

moment of inertia (less than $1.7 \times 10^{-4} \text{kgm}^2$). The fingertip force that the finger should generate varies in general from 0 to 5N. This implies that the joint acceleration can easily go up to $2 \times 10^3 \text{rad/s}$ and that the gravitational effect can be neglected in equation 1.

In the context of grasping and dexterous manipulation, most of actions (grasping, rolling, sliding, gaiting) can be done by quasi-static movements of the fingertips. Consequently, the inertia, Coriolis and viscous friction terms in equation 1 can also be neglected. Under these two hypothesis, the equation 1 becomes:

$$\tau_a - \tau_{fr} = \mathbf{J}^t \mathbf{F}_c \quad (2)$$

As stated in section I, there is usually backlash in the joints with double acting N-type tendon driving system. This system needs pre-tensioning units be installed to keep the tendon on the pulley [4], [8]. Figure 2 shows a simplified functioning model of such units.

In these systems, the springs (pre-tensioning units) are very compliant and have no other objective but keeping the tendon on track. Depending on the tendon path length variation, the backlash could range from insignificant to very large: in order to change the applied joint torque from an infinitesimal positive value (figure 2(b)) to an infinitesimal negative value (figure 2(c)), the motor must run a very long distance.

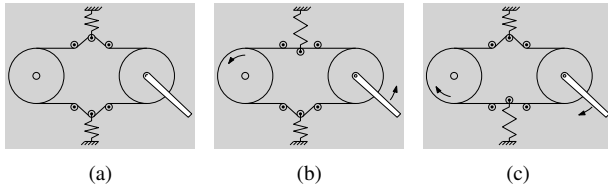


Fig. 2. Pre-tensioning units

III. FORCE CONTROL: CLASSICAL APPROACHES

In grasping and dexterous manipulation, force control plays an important role: from simply maintaining the contact forces smaller than a certain threshold to actively adjusting the fingertip force to translate and rotate an object [9], [10]. In this paper, we concentrate our efforts on the fingertip force control in the situation where the fingertip is in contact with an object and the finger-object friction prevents the fingertip from moving. In this case, all desired forces F_d can theoretically be precisely controlled as long as they stay in the frictional cone (figure 3(a)).

In the literature, there are two main approaches to realize a force controller: torque-based force control and position-based force control.

A. Torque-based force control

Torque-based force control is a force control class in which the controller directly gives the set points to joint-torque control loops or directly sets the motor currents. Resolved-acceleration-motion force control [11], [12] is a typical example. Even if theoretically straight-forward, this

method suffers from different drawbacks: the dynamic model of the system must be precise, the actuating torque must be accurate, the computational load could be heavy at high frequency. And the fact that the anthropomorphic robot hand in this study has low communication bandwidth, low computation power and significant backlash in actuator system¹ makes it difficult to smoothly control the system by torque. Indeed, as the joint acceleration α could go up to 2000rad/s^2 , during a time step $T_s \sim 10 \text{ms}$, the joint deviation could go up to $\frac{1}{2} \alpha T_s^2 = 0.1 \text{rad}$. This can put the robot in an unstable state with strong vibrations.

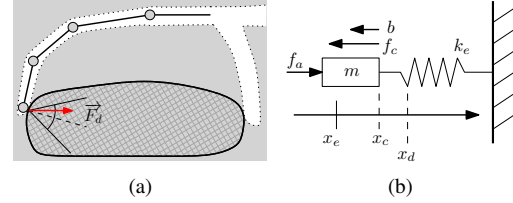


Fig. 3. A finger in interaction with an object (a) and a simplified 1D model of the interaction (b).

B. Position-based force control

Another approach which is very popular for industrial manipulators and non-direct-drive robots is position-based force control. In place of directly commanding the joint torques, the controller sends set-points to the internal joint position control loops at each time step. To get the insight of this method without going into computational burden, an 1D system is illustrated in figure 3(b) with m the equivalent finger mass, k_e, b the stiffness and damping coefficients of the finger-object system, f_a, f_c the actuating and contact forces, x_c, x_d the current and desired positions of the fingertip, x_e the position of the object without interaction. The position control loop is supposed to have a good dynamic response and the interaction force is approximated by a first order of position displacement $F_c = k_e(x_c - x_e)$. In this case, a proportional-integral controller $C_F(s) = k_0 \frac{s+a}{s}$ with appropriate choice of gains k_0 and a is sufficient to make the force closed loop (figure 4) stable with a good dynamic response.

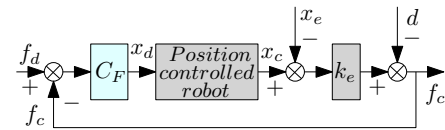


Fig. 4. Position-based force control loop in 1D case where d represents a disturbing term to the force measurements and f_d is the desired force.

However, this approach works well only on the hypothesis that the position control loop produces good performance. Yet it is not the case for our system due to backlash. Moreover, when the fingertip-object stiffness goes high ($\sim 10 \text{kN/m}$), the poor repeatability ($\sim 0.4 \text{mm}$) makes the force error easily go up to $10 \times 10^3 \times 0.4 \times 10^{-3} = 4 \text{N}$, which is already out of the functional range of the hand. This conclusion will be confirmed in section V-B.

¹which is very different from the hand DLR-HIT II [13] at these points.

C. Conclusion

The above paragraphs showed that both classical approaches failed to well control our system. The torque-based approach failed mainly because of the limit in communication frequency and computation power whereas the position-based approach failed due to the poor performance of the position control loop. This fact motivates us to take a new approach that is presented in the following section.

IV. FORCE CONTROL: NEW APPROACH

To overcome the drawbacks mentioned above, we propose a new approach based on the hypothesis presented in section II:

- Capability of the joint position control loop to reject the disturbance: when the finger is in contact with a manipulated object, the interaction force constitutes a disturbance to the joint position controllers. If this disturbance creates a non-zero error in joint position, the actuating joint torques τ_a will increase rapidly to their maximum values τ_{max} to reject this disturbance (τ_{max} is the torque saturation value).
- Quasi-static movement with negligible gravitational force: as only quasi-static movement is considered and the finger weight is negligible, the relationship between the actuating torque τ_a , the joint friction τ_{fr} and the fingertip contact force F_c can be described by equation 2.

With these two hypothesis, a new force control algorithm based on max-torque (τ_{max}) adjustment will be elaborated in the following sections. Before tackling the case of a multiple DOF² finger, the case of a single DOF finger is presented in the first place.

A. Force control of a single DOF finger

Before describing in detail the system, let's give some definitions:

Definition 4.1: Given a system S with observable variable \mathbf{Y} and actuating variable \mathbf{U} . The system is said to be locally controllable at a point $\mathbf{Y} = y_d$ if there exists a neighbourhood $\mathcal{B}(y_d)$ such that for all $y_i \in \mathcal{B}(y_d)$, there exists a control law \mathbf{U}_a such that

- $\mathbf{Y}(0) = y_i$
- $\lim_{t \rightarrow +\infty} \mathbf{Y}(t) = y_d$ when the system S is under the action of \mathbf{U}_a (t represents the time variable).

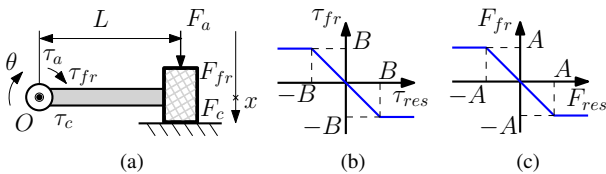


Fig. 5. (a) Force control under dry-friction, (b) torque dry-friction behaviour and (c) force dry-friction behaviour where $A = \frac{B}{L}$ and F_{res}, τ_{res} are respectively the differences between F_a and F_c , τ_a and τ_c .

²degree of freedom

Let us now consider a single DOF finger of length L rotating around O and pushing against a wall by an actuating torque τ_a (coming from the joint actuator) as shown in figure 5(a). The joint of this robot arm is not perfect and suffers from a dry friction τ_{fr} with typical behaviour given in figure 5(b) where B is the torque dry friction constant (viscous friction is omitted in this model). The actuating torque τ_a generates an actuating force $F_a = \frac{\tau_a}{L}$ at the fingertip. The dry-friction torque τ_{fr} can be equivalently modelled as if it was generated by a dry-friction force $F_{fr} = \frac{\tau_{fr}}{L}$ at that fingertip; the behaviour of F_{fr} is shown in figure 5(c) where $A = \frac{B}{L}$. The contact force F_c is measured by a force sensor and is the variable to control. The torque τ_c around O caused by this force (supposed to be perpendicular to the radius) is given by $\tau_c = \frac{F_c}{L}$. We assume here that the mass m of the finger is small, the stiffness k_e and damping b_e of the fingertip-environment pair are sufficiently high so that the dynamic effect is negligible, which means that $F_c = F_a - F_{fr}$. In this case, we can prove the following proposition:

Proposition 4.1: If the actuating torque τ_a (and then the actuating force F_a) is one-side (only push, not pull), then the system is locally controllable at a desired value F_d only when F_d dominates³ over A (or τ_d dominates over B). In this case, a closed loop with an integral controller is sufficient to make the system stable with zero steady-state error ($\tau_c \rightarrow \tau_d$ or $F_c \rightarrow F_d$ when $t \rightarrow \infty$).

Proof: For the desired force F_d , there are two cases: non-dominant ($0 < F_d < A$) and dominant ($F_d \geq A$).

1) *Non-dominant case:* In this case, the system is not locally controllable around F_d . Indeed, as $0 < F_d < A$, for any neighbourhood \mathcal{B} of F_d , there exists $F_0 \in \mathcal{B}(F_d)$ such that $F_d < F_0 < A$. When $F_c(0) = F_0$ (figure 6(a)), according to the properties of dry friction:

$$F_c = \begin{cases} F_0 & \text{for all } F_a \in [0, A + F_0] \\ F_a - A & \text{for all } F_a \in [A + F_0, +\infty) \end{cases} \quad (3)$$

This means that $F_c \geq F_0$ for all $F_a > 0$. Consequently, $F_d < F_0$ is unreachable for the system no matter how the actuating F_a is. In other words, the system is not locally controllable at F_d .

2) *Dominant case:* In this case, the system is locally controllable around F_d . Indeed, as $F_d > A$, there exists $\varepsilon > 0$ such that $F_d - \varepsilon > A$. Let's consider the neighbourhood $\mathcal{B} = (F_d - \varepsilon, F_d + \varepsilon)$ of F_d . Consider also $F_c(0) = F_0$ for any $F_0 \in \mathcal{B}(F_d)$. As $F_0 > F_d - \varepsilon > A$, according to the properties of dry friction, $F_a(0)$ must lie in the segment $\mathcal{L}_f = [F_0 - A, F_0 + A]$. In this situation, two cases are distinguished:

- if $F_0 > F_d$ (figure 6(b)), the following open-loop control law

$$F_a(t) = \begin{cases} F_a(0) + \frac{t}{t_0}(F_d - A - F_a(0)) & \text{for } t < t_0 \\ F_d - A & \text{for } t > t_0 \end{cases} \quad (4)$$

³Vector $\mathbf{a} = (a_i)_{i=1..n}$ is said to dominate over vector $\mathbf{b} = (b_i)_{i=1..n}$ (and denoted by $\mathbf{a} \triangleright \mathbf{b}$) if $|a_i| \geq |b_i|$ for all i .

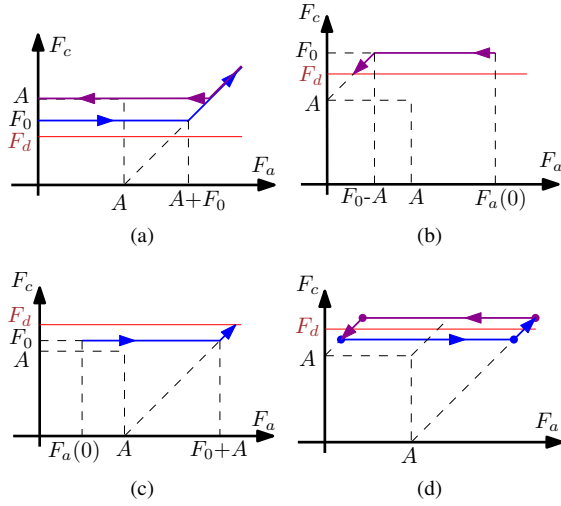


Fig. 6. 1D system responses in case of: (a) $F_d < F_0 < A$, (b) $A < F_d < F_0$, (c) $A < F_0 < F_d$, (d) $A < F_d$.

where $t_0 > 0$ is a time constant, is sufficient to make the system reach F_d .

- if $F_0 < F_d$ (figure 6(c)), the following open-loop control law

$$F_a(t) = \begin{cases} F_a(0) + \frac{t}{t_0}(F_d + A - F_a(0)) & \text{for } t < t_0 \\ F_d + A & \text{for } t > t_0 \end{cases} \quad (5)$$

where $t_0 > 0$ is a time constant, is sufficient to make the system reach F_d . The choice of t_0 depends on the rapidity of the actuating torque τ_a and depends on the desired rapidity for the force control loop.

3) *Closed loop control*: In order to enhance the robustness of the system, a closed-loop control law must be constructed. An integral controller with an appropriate gain over the above open loop system is sufficient to make the system stable with no steady state error. Indeed, when F_c is sufficiently close to $F_d > A$, the action of F_a on the system can be modelled as a simple hysteresis (figure 6(d)). Suppose that a disturbance D is present in the system as shown in figure 7, we will show that the system is stable with zero steady state error in this case. Under the action of the disturbance, the behaviour of the system when F_c is close to F_d can be modelled as shown in figure 8.

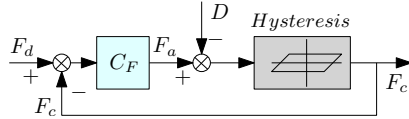


Fig. 7. Force control scheme of 1D one-side (mono directional) actuating system with dry-friction with a controller C_F .

To simplify the arguments, we consider here a time-discrete controller with sampling time T_s and an integral gain k_I of the controller C_F (figure 7) such that $k_I T_s = \alpha < 2$ for this system (the reason motivating this choice will be explained later). Suppose that at an instance $t_n = nT_s$, the current force $F_{c,n}$ is close to $F_{d,n}$. Let us denote $\varepsilon_n = |F_{d,n} - F_{c,n}|$ the absolute value of the force error

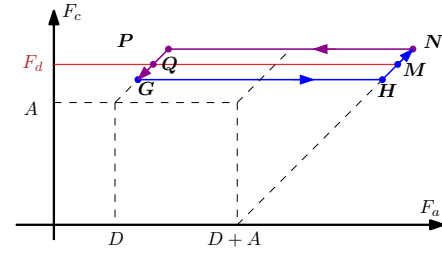


Fig. 8. 1D system behaviour in case of $F_d > A$ with disturbance D .

and $F = (F_a, F_c)$ the state of the above system. This state can be represented as a point in a plane as in figure 8. In general, there are three cases:

- **Case 1:** $F_c = F_d$. In this case, the system state F belongs to the segment MQ .
- **Case 2:** $F_c < F_d$. In this case, the system state F belongs to the segment GH .
- **Case 3:** $F_c > F_d$. In this case, the system state F belongs to the segment NP .

Case 1: This first case appears to be trivial and is not discussed in this proof.

Case 2: In this second case, $F \in GH$: as $F_{c,n} < F_{d,n}$, the integral term $I_n = \sum k_I (F_{d,n} - F_{c,n})$ increases and hence F_a . In other words, F moves in the direction G to H with a step $k_I T_s \varepsilon_n = \alpha \varepsilon_n$. After l_n steps ($l_n \leq \frac{2A}{\alpha \varepsilon_n} + 1$), F passes H and enters in the segment HN . There are two cases in this situation:

- if $\alpha \leq 1$, the system state F moves to M .
- if $1 < \alpha < 2$, there is an overshoot (F passes M) of $\varepsilon_{(n+l_n+1)} \leq (\alpha - 1)\varepsilon_n$ and the system enters in the case 3 described below.

Case 3: Almost by the same arguments as for case 2, when $F \in NP$

- the system state F moves to Q if $\alpha \leq 1$.
- there is an overshoot (F passes Q) of $\varepsilon_{(n+l_n+1)} \leq (\alpha - 1)\varepsilon_n$ after l_n steps ($l_n \leq \frac{2A}{\alpha \varepsilon_n} + 1$) if $1 < \alpha < 2$.

In conclusion,

- if $\alpha \leq 1$, F moves to M or Q . Consequently F_c converges to F_d .
- if $1 < \alpha < 2$, F turns around the segment MQ with $\varepsilon_n = |F_{d,n} - F_{c,n}|$ tends to zero as $\alpha - 1 < 1$. In other words, F_c also converges to F_d . The system is stable with no steady state error.

It is evident from the above expression that if $\alpha \geq 2$, the force error ε_n will not tend to zero. In other words, the control loop does not converge, where comes the condition $0 < \alpha < 2$ previously established. The above conclusion completes the proof. ■

B. Force control of a multiple DOF finger

Let us consider now a multiple DOF finger. In this paper, we consider only non-redundant fingers. As only 3D force control is considered, the finger is supposed to have only three DOF. Consequently, the Jacobian matrix J of the finger is a square matrix. In this part, we consider only

the configurations \mathbf{q} in which \mathbf{J} is invertible (non singular configurations). Under this hypothesis, the controller scheme presented in figure 9 where:

- k_f is a small positive scalar and the desired fingertip position \mathbf{X}_d is set to be $\mathbf{X}_d = \mathbf{X}_c + k_f \mathbf{J} \mathbf{J}^T \mathbf{F}_d$,
- \mathcal{G} and \mathcal{G}^{-1} are the forward and inverse kinematic models of the finger,
- the torque saturation τ_{max} is adjusted by a proportional-integral PI closed-loop with input \mathbf{F}_d and feedback information \mathbf{F}_c ,

is proved to give good responses when $\mathbf{J}^T \mathbf{F}_d$ dominates over τ_{fr} . The following proposition presents a theoretical justification of such a statement.

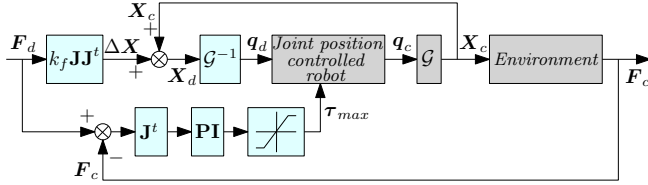


Fig. 9. Max-torque-based control loop where \mathcal{G} and \mathcal{G}^{-1} are the forward and inverse kinematic models of the finger.

Proposition 4.2: *Suppose that the vector τ_{fr} has a dry-friction behaviour with parameter \mathbf{B}_{fr} . In this case, if $\mathbf{J}^T \mathbf{F}_d$ dominates \mathbf{B}_{fr} , the controller described above is stable and has no steady-state error for an appropriate choice of gains.*

Proof: To simplify the argument, we suppose here that $\tau_{fr} > 0$. As $\mathbf{X}_d - \mathbf{X}_c = k_f \mathbf{J} \mathbf{J}^T \mathbf{F}_d$ is small in general, the following approximation can be established: $\mathbf{X}_d - \mathbf{X}_c \sim \mathbf{J}(\mathbf{q}_d - \mathbf{q}_c)$. As \mathbf{J} is invertible, the error at joint level can be approximated by:

$$\mathbf{q}_d - \mathbf{q}_c \sim \mathbf{J}^{-1}(\mathbf{X}_d - \mathbf{X}_c) = k_f \mathbf{J}^{-1} \mathbf{J} \mathbf{J}^T \mathbf{F}_d = k_f \mathbf{J}^T \mathbf{F}_d$$

which dominates over $k_f \tau_{fr} > 0$. According to the hypothesis on disturbance rejection capability of the joint controller, all actuating joint torques $\tau_a(i)$ are saturated after a short period of time and have the same sign as $\mathbf{q}_d(i) - \mathbf{q}_c(i)$ ($i = 1..n$ is the index of the joint). In other words, $\tau_a(i) = \text{sign}(\mathbf{q}_d(i) - \mathbf{q}_c(i)) \tau_{max}(i)$. In this situation, τ_{max} becomes the actuating joint torques of the finger.

It is worth noting that the action of τ_{max} is only one-side (always positive). As $\tau_d = \mathbf{J}^T \mathbf{F}_d$ dominates over τ_{fr} , the proposition 4.1 can be applied here for each joint. Consequently, $\tau_c(i) \rightarrow \tau_d(i)$ when $t \rightarrow \infty$ ($i = 1..n$) where $\tau_c = \mathbf{J}^T \mathbf{F}_c$. As \mathbf{J} is invertible, the previous statement implies that $\mathbf{F}_c \rightarrow \mathbf{F}_d$ when $t \rightarrow \infty$. In other words, \mathbf{F}_c is stable with zero steady-state error as stated in the proposition. ■

The experimental validation of this control algorithm is given in section V-C.

V. EXPERIMENTAL VALIDATION

A. Experimental platform

The platform on which our experiments were carried out consists of a finger of the Shadow motor hand [3]. It is an

anthropomorphic hand with a double-acting N -type tendon driving system (section II).

Each joint tendon is equipped with a strain gauge measuring the tendon force. The tension of each tendon is controlled by a simple PID control loop with feed-forward term running at 5kHz. The responses of this control loop are rapid when the initial state and the desired value are of the same sign (~ 40 ms). In this situation, no backlash disturbs the system. When the initial state and the desired value are of opposite signs, the responses of this loop are slow (~ 115 ms). In this situation, the motor has to move a long distance (backlash) in order to attain the desired value. This delay depends moreover on the configuration of the hand (as the backlash can vary from small to large).

The joint position control scheme is composed of two levels: velocity level and position level. The controller at velocity level is a PID and the one at position level is a PI. This joint position control loop runs at a frequency of 1kHz. Due to backlash, a dead-zone has been put in each control level. The objective of these dead-zones is to stop the motor from rewinding when the joint is "sufficiently" close to the desired position, making the system more energy efficient. However, these dead-zones reduce the precision of the control loop. The steady-state error of this control loop is typically 0.005 rad (0.3°). This implies that the precision at fingertip that these controllers can realize is about 1mm.

The fingertip is equipped with a light weight (< 10 g) force sensor ATI Nano 17 with force resolution less than 0.02N [14]. A specific algorithm is also implemented using this sensor to localize the contact position. However, in this paper, only the 3D force information of this sensor is used.

In all the experiments that follow, the finger is in contact with a fixed object as shown in figure 10. The desired force directs toward the object center (inside the friction cone) so that no sliding occurs.



Fig. 10. Force control experiments.

B. Classical position-based force control

In order to compare the performance of the proposed approach with other approaches, we present in this section the experimental results of the classical position-based approach implemented in the Shadow robot finger. The control scheme of this position-based approach is presented in figure 11 where \mathcal{G} and \mathcal{G}^{-1} are the robot forward and inverse kinematics, \mathbf{K}_e is the contact stiffness matrix and the controller is a PI with integrator of forward type: $C_F(z) = k_p + k_i \frac{T_s}{z-1}$ (T_s is the sampling period of the control loop).

Typical responses of this control loop are presented in figure 12. Observing these responses, it is worth noting that:

- Even though the responses are around set-point values, the precision is still low (~ 0.2 N).

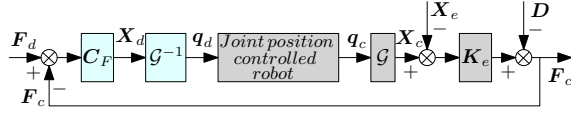


Fig. 11. Position-based force control loop in case of a robot finger.

- Some sharp drops in force responses regularly occur.

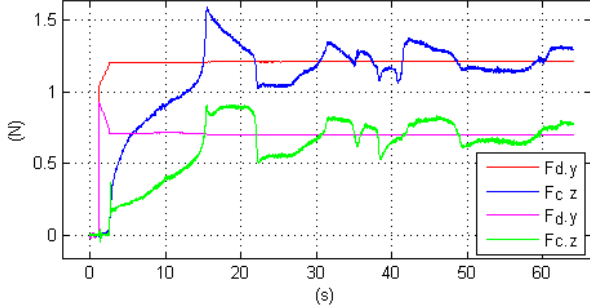


Fig. 12. Position-based force responses of the Shadow robot finger in contact with a rigid object ($F_{d,y}$, $F_{d,z}$ are desired forces in the direction O_y , O_z of the palm frame whereas $F_{c,y}$, $F_{c,z}$ are the corresponding responses). The sampling time T_s is 0.01s, the proportional and integral gains are set to be $k_p = 0.001$, $k_i = 0.03$.

Even though 0.2N is small, it is sufficient to make a grasped object move and oscillations can happen during dexterous manipulations.

C. Max-torque based force control

The step responses of the new control algorithm with the sampling time $T_s = 0.01s$ and the gains $k_f = 0.004$, $k_p = 10$, $k_i = 30$ are presented in figure 13. This figure

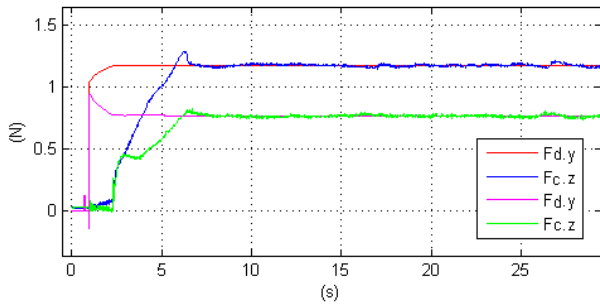


Fig. 13. Max-torque-based force responses of the Shadow robot finger in contact with a rigid object ($F_{d,y}$, $F_{d,z}$ are desired forces in the direction O_y , O_z of the palm frame whereas $F_{c,y}$, $F_{c,z}$ are the corresponding responses).

confirms the statement in proposition 4.2 that the controller has good performance when the resulting contact torques dominate over the friction torques. These responses are much better than the ones in the position-based approach and they are more adequate for dexterous manipulation tasks.

Additional experiments have been conducted with variable force set-points. These experiments are performed on two objects with a big difference in stiffness: a foam orange and a ceramic mug. The stiffness of the pair fingertip - foam orange is 400N/m and the one of the pair fingertip - ceramic mug is 27kN/m. The experimental apparatus is shown in figure 14.

In these experiments, two kinds of force set-points are sent to the system: one is of square form with $F_{max} = 1.8N$

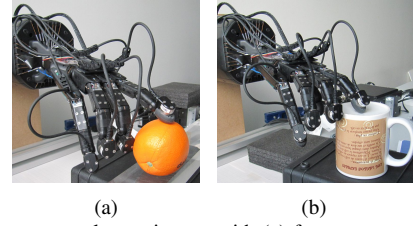


Fig. 14. Force control experiments with (a) foam orange and (b) ceramic mug.

and $F_{min} = 1.02N$, the other is of sinusoid form with $F_{max} = 1.85N$ and $F_{min} = 1.06N$. Figure 15 shows the force responses of the system in these experiments. According to the measures, the overall performance is good and the force responses succeed in tracking the set-points despite some delays. With the same set of gains k_p and k_i , the force responses for the foam orange are only slightly slower than those for the ceramic mug despite the big difference in stiffness.

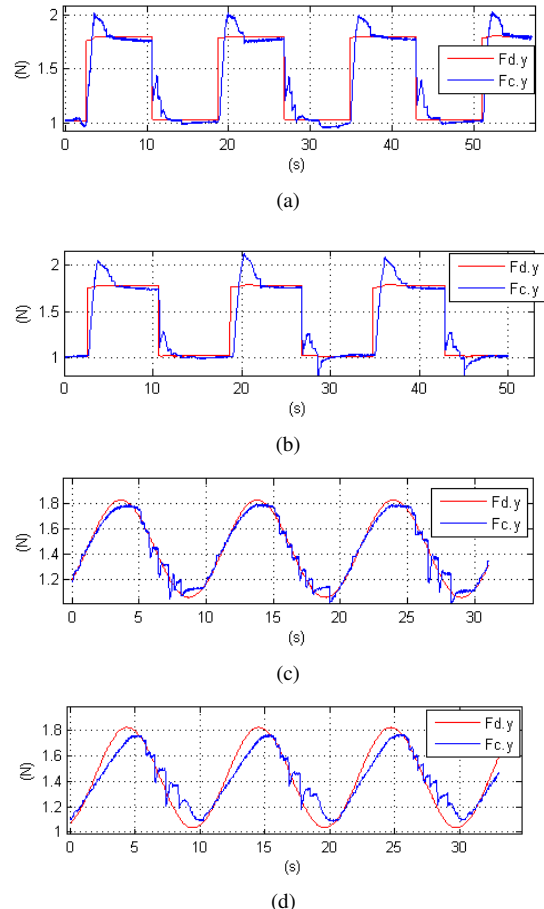


Fig. 15. Force responses for the ceramic mug (a)(c) and for the foam orange (b)(d).

It is worth noting that the square responses are asymmetric. In the rising side, they constitute a regular smooth slope with overshoot. In the decreasing side, there are stiff falls followed by small-sloped falls. These behaviours are mainly due to the fact that when the joint torque saturation τ_{max} (figure 9) increases, it takes some time to make the current joint torque τ_c attain this limit whereas when τ_{max} decreases

and τ_c is already saturated, τ_c is reduced to τ_{max} almost right away. The second factor is that the tendon dry friction becomes dominant when the actuating torque τ_c becomes small. As dry friction is not always regular, some stiff falls occur in the decreasing side. Almost the same phenomenon occurs in the sinusoid case as shown in figures (c) and (d).

VI. APPLICATION

In this section, a direct application for grasping and dexterous manipulation of the max-torque based force control scheme is presented. In this application, two controlled robot fingers hold an object and rotate it around a predefined axis.

Moving objects via fingertip contacts can be done by many different methods roughly divided into two groups: impedance control [15] and hybrid control ([16], [9]). The impedance approach is more stable but fails to precisely control the contact forces. The hybrid approach is more precise but requires complex algorithms to coordinate the fingertip force set-points.

In this application, to simplify the calculation, a pseudo stiffness control is built based on the fingertip force controller presented above. In this control scheme, the desired force F_d is generated based on the position of the fingertip relative to a certain point X_0 and a predefined stiffness k . In other words, $F_d = k(X_c - X_0)$ where X_c is the current fingertip position in world coordinates. By properly adjusting X_0 and k , the object can be stably held between two fingers and moved along a desired trajectory. In this part, only a rotation around the vertical axis is done (figure 16). The video submitted along with this paper better illustrates the movements as well as the applied forces.

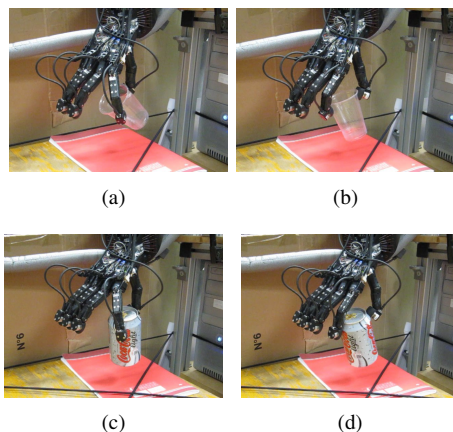


Fig. 16. Rotation of a plastic goblet (a)(b) and a coke can (c)(d)

This application shows that even though the control scheme is simple, it is very efficient in object grasping and rotating. It can potentially be used for other actions (translating, finger gaing and sliding) in dexterous manipulation tasks. These experiments are not intended to exclusively compare different types of force controllers but to show that the max-torque based force controllers can be used for dexterous manipulations and that they have good performance for varying force set-points.

VII. CONCLUSION AND FUTURE WORKS

With a new approach based on max-torque adjustment, we succeeded in controlling the 3D fingertip force of an anthropomorphic hand with a double-acting N -type tendon driving system. The experimental results performed on an anthropomorphic robot hand show rapid and precise responses even when the position control produces a poor performance. On the one hand, the success of this algorithm will enable many other advances in the domain of grasping and dexterous manipulation. On the other hand, this new approach has strong potential to be generalized to other systems and other force control tasks (hybrid position-force control in particular).

ACKNOWLEDGMENTS

The authors gratefully acknowledge Dr. Guillaume Walck for his technological expertise and the Shadow company for their technical support.

REFERENCES

- [1] D. Whitney, "Historical perspective and state of the art in robot force control," in *Robotics and Automation. Proceedings. 1985 IEEE International Conference on*, vol. 2, mar 1985, pp. 262 – 268.
- [2] J. De Schutter, et al., "Force control: A bird's eye view," in *In B. Siciliano (Ed.), Control Problems in Robotics and Automation: Future Directions*. Springer Verlag, 1997, pp. 1–17.
- [3] Shadow-Robot-Company, "Shadow motor hand," www.shadowrobot.com, 2011.
- [4] C. Melchiorri and M. Kaneko, *Robot Hands*. Springer Berlin / Heidelberg, 2008, ch. 15, pp. 345–360.
- [5] C. Melchiorri and G. Vassura, "Mechanical and control features of the university of bologna hand version 2," in *Intelligent Robots and Systems, 1992., Proceedings of the 1992 IEEE/RSJ International Conference on*, vol. 1, jul 1992, pp. 187 –193.
- [6] J. K. Salisbury and J. J. Craig, "Articulated hands: Force control and kinematic issues," *The International Journal of Robotics Research*, vol. 1, no. 1, pp. 4–17, 1982.
- [7] A. Caffaz, G. Cannata, G. Panin, G. Casalino, and E. Massucco, "The dist-hand, an anthropomorphic, fully sensorized dexterous gripper," in *IEEE-RAS International Conference on Humanoid Robotics*, September 2000.
- [8] R. Walker, A. De La Rosa, H. Elias, M. Godden, and J. Goldsmith, "Advances in actuation technology for compliant dexterous manipulation," in *Robotics and Biomimetics (ROBIO), 2010 IEEE International Conference on*, dec. 2010, pp. 1429 –1433.
- [9] V. Perdereau and M. Drouin, "Hybrid external control for two robot coordinated motion," *Robotica*, vol. 14, pp. 141–153, 1996.
- [10] T. Yoshikawa, "Multifingered robot hands: Control for grasping and manipulation," *Annual Reviews in Control*, vol. 34, no. 2, 2010.
- [11] K. G. Shin and C.-P. Lee, "Compliant control of robotic manipulators with resolved acceleration," in *Decision and Control, 1985 24th IEEE Conference on*, vol. 24, dec. 1985, pp. 350 –357.
- [12] F. Caccavale, C. Natale, B. Siciliano, and L. Villani, "Resolved-acceleration control of robot manipulators: A critical review with experiments," *Robotica*, vol. 16, no. 5, pp. 565–573, Sept. 1998.
- [13] Z. Chen, N. Lii, T. Wimboeck, S. Fan, M. Jin, C. Borst, and H. Liu, "Experimental study on impedance control for the five-finger dexterous robot hand dlr-hit ii," in *Intelligent Robots and Systems (IROS), 2010 IEEE/RSJ International Conference on*, 2010, pp. 5867–5874.
- [14] ATI-Industrial-Solution, "6-axis force sensor nano 17," <http://www.atia.com>, 2011.
- [15] S. Schneider and J. Cannon, R.H., "Object impedance control for cooperative manipulation: theory and experimental results," *Robotics and Automation, IEEE Transactions on*, vol. 8, no. 3, pp. 383 –394, jun 1992.
- [16] T. Yoshikawa and X. Zheng, "Coordinated dynamic hybrid position/force control for multiple robot manipulators handling one constrained object," in *Robotics and Automation, 1990. Proceedings., 1990 IEEE International Conference on*, may 1990, pp. 1178 –1183 vol.2.